Full title: Effects of unilateral cortical resection of the visual cortex on bilateral human white matter

Short running title: Effects of resection on white matter

Anne Margarette S. Maallo[1,2], Erez Freud[1,3,4], Tina Tong Liu[1,5], Christina Patterson[6], Marlene Behrmann[1,2]

[1] Department of Psychology, Carnegie Mellon University, Pittsburgh, PA, USA

[2] Center for the Neural Basis of Cognition, Pittsburgh, PA, USA

[3] Department of Psychology, York University, Toronto, ON, Canada

[4] Center for Vision Research, ON, Canada

[5] Laboratory of Brain and Cognition, National Institutes of Health, Bethesda, MD

[6] Department of Pediatrics, University of Pittsburgh, Pittsburgh, PA

Correspondence: Anne Margarette S. Maallo, Ph.D.

Email: maallo@cmu.edu

Department of Psychology

Baker Hall 331G

Carnegie Mellon University

5000 Forbes Ave., Pittsburgh PA, 15213

Abstract

Children with unilateral resections of ventral occipito-temporal cortex do not necessarily evince visual perceptual impairments, even when category-selective regions are resected. We aim to elucidate the extent to which bilateral cortical white matter is affected by the focal resection in search of possible explanations for the apparent behavioral competence. In order to uncover both local and broader resection-induced changes, we analyzed tractography data from eight children with unilateral cortical resections and 15 age-matched controls using two complementary approaches. First, we used a deterministic fiber tracking algorithm to define the two major white matter pathways in the visual cortex that connect the occipital and temporal lobes: the inferior longitudinal and inferior fronto-occipital fasciculi. We then compared the microstructural indices of the tracts in the patients to the controls, and found that group differences were restricted to the ipsilesional hemisphere in the patients. Single-subject analyses showed further that these differences were evident only in the site of the resection. Second, we characterized the connectivity of the contralesional hemisphere's occipito-temporal cortex using network analysis and found that, consistent with the normal microstructural indices of the contralesional fasciculi, there were no changes to the contralesional networks in patients with resections to their left visual cortex. Interestingly, while the integrity of specific tracts was intact, we found altered network properties in two patients with resections to their right visual cortex. Our results suggest first, that in cases of cortical resection during childhood, the microstructural damage to white matter is specific to the site of the resection without anterograde degeneration of the tracts; second, that hemispheric lateralization might be key to differential changes to the contralesional network organization; and last, that a unilateral network of regions with intact structural connectivity might be sufficient to subserve normal visual perception.

Keywords

white matter tractography, graph theory, lobectomy, visual cortex

Abbreviations

AD axial diffusivity

DNET dysembryoplastic neuroepithelial tumor

FA fractional anisotropy

IFOF inferior fronto-occipital fasciculus

ILF inferior longitudinal fasciculus

LH left hemisphere

RD radial diffusivity

RH right hemisphere

ROI region of interest

VOTC ventral occipito-temporal cortex

1 Introduction

Recent studies have revealed that visual perception is intact in most pediatric cases of unilateral cortical resections following ventral occipito-temporal cortex (VOTC) as a result of medically refractory epilepsy. A longitudinal study of one such case, UD, demonstrated eventual normal organization in the contralesional hemisphere following surgical removal of the VOTC in the right hemisphere (RH), (Liu *et al*., 2018). Despite the large extent of the resection that resulted in a persistent hemianopia and affected some category-selective regions in the RH (e.g. fusiform face area), UD exhibited normal visual perception. These findings of preserved visual function and abilities were corroborated in a larger group of children, with the exception of those with neurological comorbidities (Liu *et al*., 2019).

A critical question concerns the specific nature of the neural changes that support the intact perceptual abilities in these patients. One possible mechanism that might impact functional outcome is the changes in connectivity and network properties of the cortex postoperatively. Indeed, decades of research has pointed to cortical expansion and displacement mechanisms (Kaas, 1991; Eysel and Schweigart, 1999) and increased efficacy of excitatory horizontal axons (Charles, 1995; Darian-Smith and Gilbert, 1994) as key to predicting recovery in sensory and motor cortices in non-human primates following direct damage. Recently, in humans, data obtained from neuroimaging, combined with network approaches (Sinha *et al*., 2017; Zhang *et al*., 2018), have been increasingly used to predict functional outcome in epileptic children postoperatively (Paldino *et al*., 2017b,c 2019). Of note is that network properties not only capture biologically and psychologically relevant measures in the pediatric epileptic brain cross-sectionally, but are highly replicable longitudinally (Paldino *et al*., 2017a).

Concurrently, there has also been detailed examination of the modifications of structural connectivity in the pediatric epileptic population postoperatively. For example,

changes in microstructural properties of specific fiber tracts have been associated with clinical phenotype in patients with language impairments (Paldino *et al*., 2014b) and network properties estimated from structural connectivity have been used to classify epileptic and non-epileptic groups with high accuracy (Ghazi and Soltanian-Zadeh, 2016). Last, structural connectivity patterns in these patients revealed alterations in network properties that extended beyond the temporal lobe and affected the default mode network, as well (Desalvo *et al*., 2014).

As evident, some structural imaging studies have successfully uncovered atypicalities in white matter and linked these alterations to functional outcomes. Here, in light of the previous findings of the sufficiency of a single hemispheric visual system for normal perception (Liu *et a*l., 2018, 2019), we explored possible changes in white matter following cortical resection of the VOTC with two complementary approaches. We acquired diffusion MRI data from six patients with unilateral resections to their VOTC, as well as in two patients with unilateral resections outside their VOTC, and in 15 age-matched non-neurological controls. First, we used tractography and tensor-derived metrics to examine the local effects of focal cortical resection on specific fiber tracts. Second, we adopted a network approach to determine whether there were broader resection-induced changes to the connectivity of the different regions in the occipito-temporal cortex.

2 Materials and Methods

2.1 Participants

Six pediatric patients with resections to the VOTC and two patients with resections outside the VOTC, and 15 age-matched typically-developing controls (three female, 12 male, mean age 14.5 ± 3.1 years; no age difference across groups, Wilcoxon rank sum test $p>0.67$), participated in the study. In seven patients, surgery was performed to manage medically

refractory epilepsy while one patient had an emergent evacuation of cerebral hematoma at day one of life (Table 1).

All participants completed several tasks to assess their visual perception (Liu *et al*., 2018, 2019). Briefly, participants completed two tasks assessing their global perception: one that evaluates contour integration and one that measures their ability to detect 'swirl' in Glass patterns. Two further tasks examined their pattern recognition; one designed to assess object perception and one to measure face recognition. The findings of these tasks are included in Table C1 (see Supplementary Material for details). Only patient NN was impaired relative to the controls and this was true both for the global perception and pattern recognition tasks.

The procedures were reviewed and approved by the Institutional Review Boards of Carnegie Mellon University and the University of Pittsburgh. Parents gave informed consent and minor participants gave assent prior to the scanning session.

2.2 MRI Protocols

Images were acquired on a Siemens Verio 3T scanner with a 32-channel head coil at Carnegie Mellon University. T_1-weighted images with $1\times1\times1mm^3$ resolution (MPRAGE, TE=1.97ms, TR=2300ms, acquisition time=5m21s) and diffusion-weighted images with $2\times2\times2mm^3$ resolution (2D EPI, 113 directions, maximum b=4000s/mm^2, TE=121ms, TR=3981ms, acquisition time=7m46s) were acquired for all participants.

2.3 Comparison of VOTC white matter pathways between patients and controls

This first approach allowed us to determine whether there were local alterations to either of two major white matter tracts in the VOTC. The first pathway, the inferior longitudinal fasciculus (ILF), connects the occipital and temporal lobes. The second pathway,

the inferior fronto-occipital fasciculus (IFOF), is an indirect pathway between the occipital and frontal lobes that traverses the temporal lobe.

The diffusion data were reconstructed using generalized q-sampling imaging (Fang-Cheng Yeh *et al*., 2010) with 1.25 diffusion sampling ratio. We used a deterministic fiber tracking algorithm (Yeh *et al*., 2013) with whole-brain seeding, 0.20 quantitative anisotropy threshold, 0.20mm step size, 20mm minimum length, and 150mm maximum length to generate four sets of tractograms with one million streamlines each, at angular thresholds of 30°, 40°, 50°, and 60° that were ultimately combined to create one effective whole-brain tractogram. These thresholds were consistent with values used in literature (Dennis *et al*., 2015) that allow for robust fiber tract reconstructions.

Next, we delineated the ILF and IFOF in the patient group, in both the ipsilesional and contralesional hemispheres, as well as in both hemispheres of the control group. We filtered the global tractogram described above to extract the tracts using the following procedure, which has been previously used successfully to generate reproducible results (Wakana *et al*., 2007). The ILF was defined using two regions of interest (ROIs) as inclusion masks. One ROI included the entire occipital cortex and was located coronally at the most anterior slice of the parieto-occipital sulcus. The other ROI included the entire temporal lobe and was located coronally at the most posterior slice in which the temporal lobe was detached from the frontal lobe. The IFOF was defined similarly: one ROI included the entire occipital cortex and was located coronally halfway between the anterior and posterior slices of the parieto-occipital sulcus. The other ROI included the entire frontal lobe and was located coronally at the anterior edge of the genu of the corpus callosum. For both tracts, streamlines that projected across the midline were discarded.

We measured the fractional anisotropy (FA), axial diffusivity (AD), and radial diffusivity (RD) of the tracts in DSI Studio (http://dsi-studio.labsolver.org). We opted to

measure only AD and RD, and not the mean diffusivity, as the two former indices offer clearer insight into the nature of injury (Aung *et al*., 2013). AD is a measure of diffusion parallel to the length of a tract and RD is a measure of the diffusion perpendicular to the length of a tract. While FA has typically been used to characterize microstructural integrity, AD and RD have been shown to be more sensitive biomarkers for white matter defects (Arfanakis *et al*., 2002; Xu *et al*., 2007; Moen *et al*., 2016), though the associated mechanisms might differ. Abnormal AD values might indicate axonal fragmentation, resulting in restricted diffusion along the principal direction and abnormal RD values might indicate compromised bundle integrity that allow diffusion out of the white matter bundle. AD has been shown to either increase (de Ruiter *et al*., 2011; Della Nave *et al*., 2011; Zhu *et al*., 2013; Counsell, 2006; Acosta-Cabronero *et al*., 2010) or decrease (Budde *et al*., 2009; Kubicki *et al*., 2013) in response to white matter pathology. [On the other hand, for studies that did not find significant changes in AD in cases of white matter abnormalities, see (Via *et al*., 2014; Akhlaghi *et al*., 2014)]. While changes in AD are more variable, an increase in RD is typically attributed to demyelination (Song *et al*., 2002, 2005).

Profiles of the microstructural indices were obtained along the anteroposterior direction. To quantify any abnormalities, we computed the mean microstructural indices in two regimes. In the first regime, we computed the mean indices over the entire length of each tract and used these values in between-group comparisons. In the second regime, we computed the mean indices over segments of each tract and used these values in single-subject analyses. Given the heterogeneity in the resection site in the patients, we deemed it sufficient to divide the tracts into two segments, based on the generally large extent of the resections, thus, resulting in anterior and posterior segments of equal length that varied for each tract in each individual.

2.4 Characterizing the network properties in the contralesional hemisphere

This second approach allowed us to determine whether there were broader resection-induced changes in the connectivity of regions in the occipito-temporal cortex that might be related to the largely intact visual performance in such patients. We elected to study only the contralesional hemisphere network for several reasons. First, the heterogeneity in the location and extent of the resection in the patients and the variability in the preserved ipsilesional tissue made it difficult to study the ipsilesional hemisphere across the group. Additionally, automated parcellation of the ipsilesional hemisphere was likely to be unreliable given the structural abnormalities and manual demarcation of regions may not be sufficiently systematic across cases.

For each participant, we used only a single tractogram to define the network connectivity, with an angular threshold of 60°. All other thresholds were the same as in Section 2.3, except the number of streamlines. We controlled for the variability in brain sizes in our participants by keeping the seed density (20/voxel) constant across individuals, thus controlling for seeding effects on tractography (Cheng *et al*., 2012), and generated a set of tractograms by placing seeds only in a mask encompassing the preserved hemisphere.

We used cortical ROIs based on the parcellation of the anatomical images using the Destrieux atlas (Destrieux *et al*., 2000) in FreeSurfer (Dale *et al*., 1999). The parcellation output was visually inspected and confirmed to be reliable in the structurally preserved hemisphere of the patients. See supplementary materials for list of the regions comprising the occipito-temporal cortex that were used as network nodes. We generated a connectivity matrix in DSI Studio, such that, for any ROI pairs, the connectivity value was the mean FA of all tracts that pass through both ROIs. We binarized the connectivity matrix for each individual by having a threshold of one standard deviation below the mean FA (excluding FA values of 0). Any value higher than the threshold was assigned a value of 1, and every other

value was assigned a value of 0. With this binary connectivity matrix, we computed four network measures: transitivity, modularity, characteristic path length, and global network efficiency using the Brain Connectivity Toolbox (Rubinov and Sporns, 2010) for MatLab. We then compared these graph-theoretic measures between patients and controls using single-subject analyses.

We measured transitivity and modularity (as these reflect segregation of the nodes into sub-networks) and characteristic path length and efficiency (as these reflect the ease of information flow in the network) (Bullmore and Sporns, 2009; Rubinov and Sporns, 2010; Paldino *et al*., 2019). Transitivity is a measure of completely connected triangles within a network (Paldino *et al*., 2017b) and modularity is a measure of the tendency of nodes to form independent modules within the network (Zhang *et al*., 2018). That is, within the occipito-temporal cortex, one possible motif of reorganization is altered connectivity between specific regions and/or groups of regions. Characteristic path length is the minimum number of edges that indirectly connect any node to another (Bullmore and Sporns, 2009), and efficiency is simply the inverse of the mean path length. Now, it is possible that efficiency might decrease (and path length might increase) if pruning of the initially overabundant connections (Low and Cheng, 2006) is arrested because of the resection, thus leaving intact some sub-optimal white matter pathways. Alternatively, the efficiency might increase if axonal sprouting occurred as in (Dancause *et al*., 2005), and fostered the wiring of “detour circuits” (Chen and Zheng, 2014).

2.5 Statistical analyses

2.5.1 Group comparisons

In the between-group comparisons, given the small number of VOTC resection patients, we generated 100,000 permutations of data from the two groups (six patients and 15

controls) and used a two-sample t-test, thus creating a null distribution of t-scores. p-values were computed as the ratio of values more extreme than the actual group differences to the number of permutations (the number of $|t|>t_{actual}$ divided by 100,000).

2.5.2 Single-subject level comparisons

In the single subject analyses, we used established statistical procedures (Crawford and Howell, 1998) to compare each individual patient's data to the data from a small group of normative controls. With a small normative sample size, a modified t-test was used in which each patient was treated as a sample of n=1, thereby eliminating the contribution of the single subject to the estimate of within-group variance.

2.6 Data Availability

The data presented here are available from the corresponding author on request.

3 Results

3.1 ILF and IFOF damage is confined to the extent of the resection

We defined the ILF and IFOF in six children with unilateral resections to their VOTC. These tracts were chosen because they typically course through both the occipital and temporal lobes and are known to mediate visual perception (Mishkin *et al.*, 1983). We were able to reconstruct the ILF and the IFOF in most patients, even in the ipsilesional hemisphere (Fig. 1), with the exception of the ipsilesional ILF and IFOF in KQ and the ipsilesional IFOF in SN. This was unsurprising given the extent of resection that affected the anterior temporal lobe in these patients, thereby preventing us from accurately drawing the ROI to delineate the

tracts. Moreover, the large resections caused the automated tractography to fail in distinguishing pathways that passed the quantitative thresholds, as voxels containing cerebrospinal fluid, which now occupied the resection site, have different diffusion values to voxels containing white matter.

3.1.1 Between-group differences in microstructural properties of the tracts

To conduct quantitative evaluation of any differences between patients and controls, we computed the mean FA, AD, and RD in each of the identified tracts. The specific indices were chosen because they offer a mechanistic relationship to the nature of injury (Aung *et al*., 2013). Generally, high FA indicates good tract integrity (streamlines follow coherent orientation) and high AD and high RD might indicate axonal fragmentation and demyelination, respectively.

We compared both the ipsilesional and contralesional tracts in patients to the tracts from either hemisphere in controls. Because we combined all patients with resections in either hemisphere, we also compared the microstructural indices in patients to the mean of the bilateral tracts in controls (Fig. 2). We found that, for the ipsilesional ILF, FA was lower and both AD and RD were higher in patients than controls (all $|t|>2.5$, all $p<0.01$). Meanwhile, for the ipsilesional IFOF, only RD exhibited significant differences between patients and controls (RD was higher in patients, $t=2.5$, $p<0.05$). In contrast, for all indices, the findings for both the contralesional ILF and IFOF did not differ significantly between the patients and the controls (all $|t|<1.69$), all $p>0.11$). Moreover, these results converged irrespective of whether the pooled patient data were compared to data from either hemisphere in controls, or to the mean of the bilateral tracts in controls.

3.1.2 Qualitative within-subject hemispheric asymmetry in microstructural properties of the tracts

Next, we wished to determine whether the observed ipsilesional group differences were diffuse along the entire length of the tracts, or restricted to the proximate site of the resection. We first provide a qualitative analysis and, thereafter, report the quantitative findings. We plotted the different microstructural indices along the anteroposterior axis of the ILF (Fig. 3A) and the IFOF (Fig. 4A). Qualitatively, in an exemplar control participant (top rows, Fig. 3A and Fig. 4A), the respective microstructural indices of the bilateral ILF and the bilateral IFOF were equivalent along the entire length of the two tracts.

Unlike controls, in patients with bilateral ILF, there were within-subject differences in the microstructural indices of the two hemispheres (preserved hemisphere serves as within-subject comparison, Fig. 3A): FA was lower, and AD and RD were higher in the ipsilesional than in the contralesional ILF. Furthermore, these differences appeared to be confined to the extent of the resection of each patient. In patients SN and OT with anterior temporal lobe resections, the within-subject hemispheric asymmetry was evident mostly in the anterior segment of the ILF only. While in patients UD, TC, and NN, who had more posterior resections, the within-subject hemispheric asymmetries appear to be restricted to the posterior segment of the ILF.

The anteroposterior profiles of microstructural indices of the IFOF is also different to those of controls, as well as to the profiles of the same measures in the ILF. Within-subject hemispheric differences in the IFOF were seen only in patients with more posterior VOTC resections (Fig. 4A) in whom FA was lower, AD and RD were higher in the ipsilesional than in the contralesional IFOF. However, the IFOF could not be defined in two of the three patients with anterior resection and so this finding ought to be interpreted with caution. Last, in one unique patient, OT, with a preserved medial temporal lobe, there were no qualitative

within-subject hemispheric asymmetries. This is unsurprising as the IFOF extends from the occipital lobe to the frontal lobe, grazing only the medial and not the lateral temporal lobe (Makris *et al*., 2007).

3.1.3 Quantitative single-subject level changes in microstructural properties of the tracts

We next quantified the hemispheric asymmetry in the microstructural indices evident in the anteroposterior profiles in patients compared to controls by comparing the mean microstructural indices of all tract segments in patients to the corresponding values from controls (ILF: Fig. 3B and IFOF: Fig. 4B). On an individual level, consistent with the group permutation results, the differences between patients and controls were a result of compromised ipsilesional tracts. Aside from patient OT, who exhibited normal microstructural indices across the board, we found that FA was lower and both AD and RD were higher in the ipsilesional than the contralesional ILF. Critically, the damage to the tract was confined to the extent of the resection (Fig. 3B, all $|t|>2.4$, all $p<0.05$). That is, patients with posterior resections had compromised microstructural indices only in the posterior segment of the ILF and patient SN (the only patient who had an anterior resection with bilaterally defined ILF) exhibited compromised microstructural indices only in anterior microstructural indices of the ILF. As for the IFOF, consistent with the qualitative assessment, only the patients with posterior resections exhibited compromised microstructural indices in the posterior segment of the IFOF (Fig. 4B, all $|t|>2.3$, all $p<0.05$).

3.1.4 Patients with resection outside VOTC had normal microstructural properties of the tracts

Thus far, we have demonstrated alterations to the microstructure of the ipsilesional tracts in VOTC in the patients (except OT) and have proposed that these changes are a direct product of the resection. An alternative possibility, however, is that the abnormalities might not be a consequence of the resection, but instead a manifestation of overall white matter deterioration concomitant with the etiology that prompted surgery in the first place. To validate this, we characterized the ILF and IFOF (Fig. 5A) in two patients with medically refractory epilepsy and resections outside their VOTC. If the damage observed in the six VOTC patients was a result of the resection, then there should be no abnormalities in the ILF and IFOF of the two patients with resections outside the VOTC, given the distal location of the tracts with respect to their resection. Using identical procedures as in the children with VOTC resections, we found no within-subject hemispheric asymmetry in the anteroposterior profiles of the microstructural indices of either tract in these two patients (Fig. 5B-C). Furthermore, single-subject analysis revealed no significant differences for any of the tract segments across any of the indices (all $|t|<1.23$, all $p>0.24$). These results reveal that the alterations observed in the VOTC resection cases are likely a specific outcome of the resection and not due to a more pervasive white matter deterioration linked to epilepsy.

Taken together, our results showed that, in children with a VOTC resection, there was well-circumscribed damage to the ipsilesional white matter that manifested in one or all of the following neuroimaging markers: there was within-subject hemispheric asymmetry in the microstructural indices – FA was lower, while both AD and RD were higher in the ipsilesional than in the contralesional tract. Moreover, this was only true in regions proximal to the resection. Distal and contralesional to the resection, the microstructural indices were normal compared to controls. That the damage remained circumscribed is illuminating and contrasts with findings of intracortical axonal degeneration ascribed to the loss of inhibition from the lesioned area in cats (Creutzfeldt *et al*., 1977).

3.2 Network properties of the contralesional occipito-temporal cortex

Above, we uncovered local changes to specific white matter tracts by demarcating microstructural deficits restricted to the extent of resection. In a complementary approach, we wished to examine whether there were broader resection-induced changes to the structural connectivity of the visual cortex.

Using network analysis, we observed a hemispheric difference in the patients with VOTC resections: whereas the four patients with LH VOTC resections had normal graph-theoretic measures, the two patients with RH VOTC resections exhibited altered network properties, relative to the controls (Table 2). KQ had higher modularity and characteristic path length and lower network efficiency (all $|t|>2.4$, all $p<0.05$) and UD had higher characteristic path length and lower network efficiency (both $|t|>2.2$, both $p<0.05$). Importantly, consistent with the results in Section 3.1.4, there were no changes to the network properties in the two patients with resections outside their VOTC, again revealing specificity of the network changes to the VOTC resection itself.

4 Discussion

Here, we characterized white matter integrity and network properties in pediatric patients with cortical resection to visual cortex as a result of medically refractory epilepsy. Intriguingly, these patients have largely intact visual perceptual function (Liu *et al*., 2018, 2019) and the question is whether alterations in white matter might underlie these positive behavioral outcomes. As has already been documented (Taylor *et al*., 2015), behavioral impairments are not always correlated with the size and site of affected cortex, and aberrant cortico-cortical interactions might affect the brain-behavior correspondence.

4.1 No anterograde degeneration of ipsilesional fiber tracts

We first characterized the ILF and IFOF, which have both previously been shown to underlie object recognition (Thomas *et al*., 2009; Tavor *et al*., 2014; Behrmann and Plaut, 2013; Decramer *et al*., 2019; Ortibus *et al*., 2011). We characterized these two tracts in six patients with unilateral resections to the VOTC, as well as in two patients with resections outside their VOTC, and compared structural characteristics with those of a matched control group. We were able to delineate all contralesional tracts and even ipsilesional tracts in most patients, except in those with extremely large resections of the entire anterior temporal lobe. The mere presence of the ipsilesional ILF and IFOF in the patients suggests that any potential damages caused by the removal of cortical tissue does not result in a cascade of axonal injury, beyond the resection site.

Within-subject hemispheric differences in FA, AD, and RD indicative of the degradation in the ipsilesional tracts were confined to the extent of resection. In the ILF, abnormalities were evident in FA, AD, and RD, while in the IFOF, abnormalities were seen only in the RD and only in individuals with posterior resections. However, a previous study has shown spurious changes to AD when, supposedly, only RD was artificially altered in simulations (Wheeler-Kingshott and Cercignani, 2009). These artifacts were due to the uncertainty in the tensor directionality and its correspondence with in vivo fiber tracts. While there does not appear to be direct post-mortem data for direct comparison with in vivo diffusion studies in children with visual system damage, the white matter perturbations seen in our patients are consistent with the effects of transection in models of spinal cord injury in rats (Siegenthaler *et al*., 2007), in that there is damage confined to the white matter near the transection site. As shown histologically, the damage in rats' spinal cords is characterized by

degradation of the myelin sheath. However, the comparison of cortical white matter damage in humans to a spinal cord injury model in animals should come with caveats. As noted in (Norenberg *et al*., 2004), the role of demyelination in human spinal cord injury is still uncertain and therefore difficult to extend to cortical axonal pathology. Nevertheless, in (Kakulas, 1999), peripheral human spinal cord white matter was determined to be relatively preserved, consistent with the presence of ipsilesional cortical tracts in our patients. Taken together, we propose that the defects in microstructure of the ipsilesional tracts following cortical resection is due to focal demyelination confined to the immediate area of the resection without anterograde degeneration of the white matter. The normal microstructural indices of the ILF and IFOF in the patients with resections outside VOTC further supports the specificity of white matter damage in the patients with focal VOTC resections.

Among the cases presented here, surprisingly, a single patient, OT, exhibited normal microstructural indices, even in the ipsilesional tracts. This cannot be simply due to the age at surgery, as other patients were either younger (SN, UD) or older (KQ, NN) at the time of resection and none showed entirely normal microstructural indices. Similarly, the normal microstructure of the tracts cannot obviously be accounted for in terms of the time when data were acquired postoperatively. One plausible explanation for the integrity of OT's tracts is etiological —OT's surgery was prompted by the presence of a dysembryoplastic neuroepithelial tumor (DNET). We speculate that the chronic growth of the DNET triggered reorganization in OT's ipsilesional hemisphere such that the white matter tracts were slowly displaced over time, and consequently, spared from damage due to the resection. However, we did not see this preservation in the only other patient with a DNET, UD, in whom we saw microstructural deficits ipsilesionally and network changes contralesionally. We do note, however, that UD's surgery occurred when he was 6 years old, but OT's surgery took place

when he was 13 years old. OT's extended preoperative development may account for the difference between him and UD. We also consider UD in further detail below (Section 4.3).

4.2 Normal visual perception despite persistent degradation in ipsilesional hemisphere

A previous longitudinal study following individuals with anterior temporal lobectomy documented changes over time to the FA of various white matter tracts, including the bilateral ILF (Li *et al*., 2019). However, the authors did not measure behavioral outcomes in these patients. In another study (Decramer *et al*., 2019), immediately after surgical removal of a left VOTC lesion, one patient had difficulty in visual processing, but full recovery was attained 1.5 years later, even with persistently damaged white matter. As we only have cross-sectional diffusion data, we cannot comment on the longitudinal variations in the microstructural damage in our patients. Nevertheless, the data used in the analyses presented here were obtained at various times postoperatively, ranging from only a few months to more than a decade, and the microstructural parameters are, nevertheless, largely similar across all the cases. It is, therefore, likely that the postoperative focal damage is persistent in these patients.

As such, our results indicate a dissociation between the postoperative structural damage and the largely normal behavioral competence in these patients. This finding is at odds with several studies reporting an association between tract degradation and visual behavioral deficits. For instance, there are cases of congenital prosopagnosia with compromised VOTC white matter pathways who, despite no obvious neurological damage and ample visual experience, do not acquire normal face recognition skills. In such individuals, the severity of the face recognition deficit was correlated with the extent to which the ILF was compromised (Gomez *et al*., 2015, Thomas *et al*., 2009; Geskin and

Behrmann, 2018). And similarly, an association between behavior and white matter has been observed in individuals who show impairments in the perception of facial emotion; moreover, the extent of the impairment was correlated with the damage to the right IFOF (Philippi *et al*., 2009).

Together, these findings support the claim that white-matter atypicalities have clear behavioral consequences. One explanation for the discrepancy between these studies and the findings we report here might be the difference in the extent of the damage along the length of tracts. Whereas the degradation of white matter associated with face processing deficits is widespread across a tract, the damage as a result of surgery in our patients is confined to the site of resection. It is also possible, albeit somewhat unlikely, that the time of the data acquisition was sufficiently long postoperatively in our cases that behavioral capabilities had recovered independent of the white matter tract status, as in the profile of full recovery of behavior, even with persistently damaged white matter (Decramer *et al*., 2019). In our cohort, only patient NN showed some intermediate and high-level visual behavioral deficits (Liu *et al*., 2019). However, it is difficult to tease this apart from other factors such as his relatively low IQ and other more widespread cortical changes resulting from the extant polymicrogyria.

An alternative explanation and one that we favor speculatively, is that the normal microstructure in the contralesional hemisphere might be evidence of "compensation" in and of itself, by the preserved hemisphere for the functions that would otherwise be mediated by the resected tissue. The cases of SN and TC with LH VOTC resections offer strong support for this view. Whereas a typical visual word form area is localized in the LH in majority of the population, in SN and TC, this region emerged in the RH, and yet, we see no enhancement of the right white matter pathways relative to controls.

Together, our findings suggest that, in the absence of bilaterally distributed category-selective regions, the intact regions in the contralesional hemisphere (Liu *et al*., 2018, 2019),

together with the normal white matter pathways in the VOTC, might suffice to support perception.

4.3 Differential effects of VOTC resection on contralesional network reorganization

In a complementary approach, using network analysis, we found that the contralesional network of the occipito-temporal cortex exhibited normal graph-theoretic measures in the two patients with resections outside the VOTC, as well as in the four patients with LH VOTC resection. On the other hand, the two patients with RH VOTC resections exhibited abnormal measures including having lower network efficiency. This result is consistent with results from a previous study that showed a decrease, albeit a moderate effect, in the network efficiency in epileptic patients (Taylor *et al*., 2018). It must be noted, however, that the result of Taylor *et al*. (2018) was based on an artificial resection on the (whole-brain) connectome data acquired preoperatively, whereas we characterized properties of the (contralesional occipito-temporal) network using in vivo data acquired postoperatively.

Given the small number of patients with VOTC resection, we cannot definitively attribute the different patterns of network organization to differences in hemispheric lateralization. Notwithstanding the limited number of patients, our findings here are provocative enough to warrant some speculation. First, we consider the normal network efficiency of the preserved contralesional hemisphere in our LH VOTC resection patients to be consistent with the normal network efficiency seen in patients with medial temporal lobe epilepsy prior to surgery (Bonilha *et al*., 2012). This suggests that there are not always changes to the network efficiency in the epileptic brain, and that any changes might be resection-induced (Taylor *et al*., 2018). Second, there is ample evidence showing hemispheric lateralization of language to the LH (Neville and Bavelier, 1998; Vicari *et al*., 2000; Josse

and Tzourio-Mazoyer, 2004) and visual function to the RH (Mcfie *et al*., 1950; Durnford and Kimura, 1971; Corballis, 2003). That we only see the changes to network properties in the two patients with RH VOTC resections might indicate white matter reorganization in the LH to better accommodate functions that are typically lateralized to, and dominant in, the RH. However, we do not see changes to the network properties in patients in whom we already know that some visual functions of the resected regions have emerged in the contralesional hemisphere (as in the right VWFA in patients SN and TC, Table 1).

Last, we note that cognitive impairments in domains that are not directly associated with visual function (e.g. IQ below 70) might be premorbidly present (Veersema *et al*., 2019) and could impact the network topography postoperatively. Nevertheless, there is one other study that showed contralesional hemisphere network changes following focal damage, even in the absence of alterations in microstructure. In (Crofts *et al*., 2011), patients exhibited within-subject hemispheric asymmetry in network communicability, as well as group-level differences relative to controls, as a result of stroke. The authors postulated that such alterations possibly reflect an adaptive mechanism. In the same vein, the changes we see to the contralesional network properties in our RH VOTC resection patients might reflect reorganization following an assault on the normal developmental trajectory of the bilateral occipito-temporal cortex. A plausible means that supports this long-distance reorganization is the corpus callosum, which plays a key role in plasticity after brain injury (Restani and Caleo, 2016) and whose maturation depends on coordinated activation across the two hemispheres (Pietrasanta *et al*., 2012). In light of this, we propose that there might be a differential effect of resection of either hemisphere on the reorganization of the contralesional hemisphere, as evident in altered network properties, but additional exploration of this issue is warranted.

While patients here all exhibited normal higher-order visual cognition (except NN), they also have different neurological profiles (Table 1). This heterogeneity confounds

determination of the relationship between network properties vis-a-vis possible compensatory behavior. Nevertheless, network properties derived from resting state data have already been shown to be reliable biomarkers even in cases of epilepsy (Paldino *et al*., 2017b). Thus, it is a worthwhile endeavor to determine whether network properties, as defined from structural connectivity, can be correlated with behavior.

5 Conclusions

We set out to determine the degree to which the white matter is altered in children with largely normal perceptual abilities and unilateral resections of visual cortical regions. We adopted two complementary approaches to probe local and broader changes. First, using tractography analysis and tensor-derived metrics to characterize specific fiber tracts, we have shown focal damage only to the ipsilesional ILF and IFOF consistent with myelin degradation. Moreover, the contralesional tracts exhibited normal microstructural indices indicating preserved white matter integrity. And second, using a network approach, we demonstrated differential effects of the resection of either hemisphere that might be related to hemispheric lateralization. This manifested in changes to the contralesional network properties of only the patients with RH VOTC resection. Despite the persistence of the alterations discovered using the two complementary approaches, there were no perceptual impairments in the patients who participated in this study (save for NN who had low IQ and extant polymicrogyria). Taken together, our findings suggest that, in cases of unilateral resections to the VOTC in childhood, the category selectivity in the preserved contralesional hemisphere, together with a structurally preserved white matter, might suffice to subserve normal visual perception.

Acknowledgments

We thank the patients, the controls, and their families for their time and cooperation. We also thank John Pyles and Tim Verstynen for helping set up the scan protocols, as well as the MRI technologists Scott Kurdilla and Mark Vignone for helping with the acquisition of the imaging data, and Frank Yeh and the VisCog group at CMU for the fruitful discussions.

Funding

This work was supported by NIH grant (RO1 EY027018) to M.B.

Competing Interests

The authors report no competing interests.

References

Acosta-Cabronero, J., Williams, G. B., Pengas, G., and Nestor, P. J. Absolute diffusivities define the landscape of white matter degeneration in Alzheimer's disease. Brain 2010; 133:529–539.

Akhlaghi, H., Yu, J., Corben, L., Georgiou-Karistianis, N., Bradshaw, J. L., Storey, E., Delatycki, M. B., and Egan, G. F. Cognitive deficits in Friedreich ataxia correlate with micro-structural changes in dentatorubral tract. Cerebellum 2014; 13:187–198.

Arfanakis, K., Haughton, V. M., Carew, J. D., Rogers, B. P., Dempsey, R. J., and Meyerand, M. E. Diffusion tensor MR Imaging in diffuse axonal injury. Am J Neuroradiology 2002; 23:794–802.

Aung, W. Y., Mar, S., and Benzinger, T. L. Diffusion tensor MRI as a biomarker in axonal and myelin damage. Imaging in Medicine 2013; 5:427–440.

Behrmann, M. and Plaut, D. C. Distributed circuits, not circumscribed centers, mediate visual recognition. Trends in Cognitive Sciences 2013; 17:210–219.

Bonilha, L., Nesland, T., Martz, G. U., Joseph, J. E., Spampinato, M. V., Edwards, J. C., and Tabesh, A. Medial temporal lobe epilepsy is associated with neuronal fibre loss and paradoxical increase in structural connectivity of limbic structures. Journal of Neurology, Neurosurgery and Psychiatry 2012; 83:903–909.

Budde, M. D., Xie, M., Cross, A. H., and Song, S.-K. Axial Diffusivity Is the Primary Correlate of Axonal Injury in the Experimental Autoimmune Encephalomyelitis Spinal Cord: A Quantitative Pixelwise Analysis. Journal of Neuroscience 2009; 29:2805–2813.

Bullmore, E. and Sporns, O. Complex brain networks: graph theoretical analysis of structural and functional systems. Nature Reviews Neuroscience 2009; 10:186–98.

Charles, D. Long-range horizontal connections and their role in cortical reorganization revealed by optical recording of cat primary visual cortex. Nature 1995; 375:780–784.

Chen, M. and Zheng, B. Axon plasticity in the mammalian central nervous system after injury. Trends in Neurosciences 2014; 37:583–593.

Cheng, H., Wang, Y., Sheng, J., Sporns, O., Kronenberger, W. G., Mathews, V. P., et al. Optimization of seed density in DTI tractography for structural networks. Journal of Neuroscience Methods 2012; 203:264–272.

Corballis, P. M. Visuospatial processing and the right-hemisphere interpreter. Brain and Cognition 2003; 53:171–176.

Counsell, S. J. Axial and Radial Diffusivity in Preterm Infants Who Have Diffuse White Matter Changes on Magnetic Resonance Imaging at Term-Equivalent Age. Pediatrics 2006; 117:376–386.

Crawford, J. R. and Howell, D. C. Comparing an individual's test score against norms derived from small Samples. The Clinical Neurophsychologist 1998; 12:482–486.

Creutzfeldt, O. D., Garey, L. J., Kuroda, R., and Wolff, J. R. The distribution of degenerating axons after small lesions in the intact and isolated visual cortex of the cat. Experimental Brain Research 1977; 27:419–440.

Crofts, J. J., Higham, D. J., Bosnell, R., Jbabdi, S., Matthews, P. M., Behrens, T. E. J., *et al*. Network analysis detects changes in the contralesional hemisphere following stroke. NeuroImage 2011; 54:161–169.

Dale, A. M., Fischl, B., and Sereno, M. I. Cortical surface-based analysis: I. Segmentation and surface reconstruction. NeuroImage 1999; 9:179–194.

Dancause, N., Barbay, S., Frost, S. B., Plautz, E. J., Chen, D., Zoubina, E. V., et al. Extensive cortical rewiring after brain injury. The Journal of Neuroscience 2005; 25:10167–79.

Darian-Smith, C. and Gilbert, C. D. Axonal sprouting accompanies functional reorganization in adult cat striate cortex. Nature 1994; 368:737–740.

de Ruiter, M. B., Reneman, L., Boogerd, W., Veltman, D. J., Caan, M., Douaud, G., et al. Late effects of high-dose adjuvant chemotherapy on white and gray matter in breast cancer survivors: Converging results from multimodal magnetic resonance imaging. Human Brain Mapping 2011; 33:2971– 2983.

Decramer, T., Premereur, E., Lagae, L., van Loon, J., Janssen, P., Sunaert, S., et al. Patient MW: transient visual hemi-agnosia. Journal of Neurology 2019; 266:691–698.

Della Nave, R., Ginestroni, A., Diciotti, S., Salvatore, E., Soricelli, A., and Mascalchi, M. Axial diffusivity is increased in the degenerating superior cerebellar peduncles of Friedreich's ataxia. Neuroradiology 2011; 53:367–372.

Dennis, E. L., Jin, Y., Kernan, C., Babikian, T., Mink, R., Babbitt, C., et al. White matter integrity in traumatic brain injury: Effects of permissible fiber turning angle. In 2015 IEEE 12th International Symposium on Biomedical Imaging; pages 930–933. IEEE.

Desalvo, M. N., Douw, L., Tanaka, N., Reisenberger, C., and Stufflebeam, S. M. Altered Structural Connectome in Temporal Lobe Epilepsy. Neuroradiology 2014; 270:842–848.

Destrieux, C., Fischl, B., Dale, A., and Halgren, E. Automatic parcellation of human cortical gyri and sulci using standard anatomical nomenclature. NeuroImage 2000; 53:1–15.

Durnford, M. and Kimura, D. Right hemisphere specialization for depth perception reflected in visual field differences. Nature 1971; 231:395–397.

Eysel, U. T. and Schweigart, G. Increased Receptive Field Size in the Surround of Chronic Lesions in the Adult Cat Visual Cortex. Cerebral Cortex 1999; 9:101–109.

Fang-Cheng Yeh, Wedeen, V. J., and Tseng, W.-Y. I. Generalized q-sampling imaging. IEEE Transactions on Medical Imaging 2010; 29:1626–1635.

Geskin, J. and Behrmann, M. Congenital prosopagnosia without object agnosia? A literature review. Cognitive Neuropsychology 2018; 35:4–54.

Ghazi, N. and Soltanian-Zadeh, H. Structural Connectivity of Temporal Lobe Structures Detects Temporal Lobe Epilepsy. In 23rd Iranian Conference on Biomedical Engineering and 2016 1st International Iranian Conference on Biomedical Engineering (ICBME), November, pages 23–25.

Gomez, J., Pestilli, F., Witthoft, N., Golarai, G., Liberman, A., Poltoratski, S., et al. Functionally Defined White Matter Reveals Segregated Pathways in Human Ventral Temporal Cortex Associated with Category-Specific Processing. Neuron 2015; 85:216–227.

Josse, G. and Tzourio-Mazoyer, N. Hemispheric specialization for language. Brain Research Reviews 2004; 44:1–12.

Kaas, J. H. Plasticity of sensory and motor maps in adult mammals. Annual Review of Neuroscience 1991; 14:137–167.

Kakulas, A. B. A review of the neuropathology of human spinal cord injury with emphasis on special features. Journal of Spinal Cord Medicine 1999; 22:119–124.

Kubicki, M., Shenton, M. E., Maciejewski, P. K., Pelavin, P. E., Hawley, K. J., Ballinger, T., et al. Decreased axial diffusivity within language connections: A possible biomarker of schizophrenia risk. Schizophrenia Research 2013; 148:67–73.

Li, W., An, D., Tong, X., Liu, W., Xiao, F., Ren, J., et al. Different patterns of white matter changes after successful surgery of mesial temporal lobe epilepsy. NeuroImage: Clinical 2019; 21:10163.

Liu, T. T., Freud, E., Patterson, C., and Behrmann, M. June 5, 2019. Perceptual function and category-selective neural organization in children with resections of visual cortex. The Journal of Neuroscience 10.1523/JNEUROSCI.3160-18.2019

Liu, T. T., Nestor, A., Vida, M. D., Pyles, J. A., Patterson, C., Yang, Y., et al. Successful reorganization of category-selective visual cortex following occipito-temporal lobectomy in childhood. Cell Reports 2018; 24:1113–1122.

Low, L. K. and Cheng, H. J. Axon pruning: An essential step underlying the developmental plasticity of neuronal connections. Philosophical Transactions of the Royal Society B: Biological Sciences 2006; 361:1531–1544.

Makris, N., Papadimitriou, G. M., Sorg, S., Kennedy, D. N., Caviness, V. S., and Pandya, D. N. The occipitofrontal fascicle in humans: A quantitative, in vivo, DT-MRI study. NeuroImage 2007; 37:1100-1111.

Mcfie, J., Piercy, M. F., and Zangwill, O. L. Visual-spatial agnosia associated with lesions of the right cerebral hemisphere. Brain 1950; 73:167–190.

Mishkin, M., Ungerleider, L. G., and Macko, K. A. Object vision and spatial vision: two cortical pathways. Trends in Neurosciences 1983; 6:414–417.

Moen, K. G., Vik, A., Olsen, A., Skandsen, T., Haberg, A. K., Evensen, K. A. I., et al. Traumatic Axonal Injury: Relationships Between Lesions in the Early Phase and Diffusion Tensor Imaging Parameters in the Chronic Phase of Traumatic Brain Injury. Journal of Neuroscience Research 2016; 635:623–635.

Neville, H. J. and Bavelier, D. Neural organization and plasticity of language. Current Opinion in Neurobiology 1998; 8:254–258.

Norenberg, M. D., Smith, J., and Marcillo, A. The Pathology of Human Spinal Cord Injury: Defining the Problems. Journal of Neurotrauma 2004; 21:429–440.

Ortibus, E., Verhoeven, J., Sunaert, S., Casteels, I., de Cock, P., and Lagae, L. Integrity of the inferior longitudinal fasciculus and impaired object recognition in children: A diffusion tensor imaging study. Developmental Medicine and Child Neurology 2011; 54:38–43.

Paldino, M. J., Chu, Z. D., Chapieski, M. L., Golriz, F., and Zhang, W. Repeatability of graph theoretical metrics derived from resting-state functional networks in paediatric epilepsy patients. British Journal of Radiology 2017a; 90:20160656.

Paldino, M. J., Golriz, F., Chapieski, M. L., Zhang, W., and Chu, Z. D. Brain network architecture and global intelligence in children with focal epilepsy. American Journal of Neuroradiology 2017b; 38:349–356.

Paldino, M. J., Golriz, F., Zhang, W., and Chu, Z. Normalization enhances brain network features that predict individual intelligence in children with epilepsy. PLoS ONE 2019; 14:e0212901.

Paldino, M. J., Hedges, K., Rodrigues, K. M., and Barboriak, D. P. Repeatability of quantitative metrics derived from MR diffusion tractography in paediatric patients with epilepsy. British Journal of Radiology 2014a; 87: 20140095.

Paldino, M. J., Hedges, K., and Zhang, W. Independent contribution of individual white matter pathways to language function in pediatric epilepsy patients. NeuroImage: Clinical 2014b; 6:327–332.

Paldino, M. J., Zhang, W., Chu, Z. D., and Golriz, F. Metrics of brain network architecture capture the impact of disease in children with epilepsy. NeuroImage: Clinical 2017c; 13:201–208.

Philippi, C. L., Mehta, S., Grabowski, T., Adolphs, R., and Rudrauf, D. Damage to Association Fiber Tracts Impairs Recognition of the Facial Expression of Emotion. The Journal of Neuroscience 2009; 29:15089–15099.

Pietrasanta, M., Restani, L., and Caleo, M. The corpus callosum and the visual cortex: Plasticity is a game for two. Neural Plasticity 2012; 2012:838672.

Restani, L. and Caleo, M. Reorganization of Visual Callosal Connections Following Alterations of Retinal Input and Brain Damage. Frontiers in Systems Neuroscience 2016; 10:86:1– 17.

Rubinov, M. and Sporns, O. Complex network measures of brain connectivity: Uses and interpretations. NeuroImage 2010; 52:1059–1069.

Siegenthaler, M. M., Tu, M. K., and Keirstead, H. S. The Extent of Myelin Pathology Differs following Contusion and Transection Spinal Cord Injury. Journal of Neurotrauma 2007; 24:1631–1646.

Sinha, N., Dauwels, J., Kaiser, M., Cash, S. S., Westover, M. B., Wang, Y., et al. Predicting neurosurgical outcomes in focal epilepsy patients using computational modelling. Brain 2017; 140:319–332.

Song, S. K., Sun, S.W., Ramsbottom, M. J., Chang, C., Russell, J., and Cross, A. H. Dysmyelination revealed through MRI as increased radial (but unchanged axial) diffusion of water. NeuroImage 2002; 17:1429–1436.

Song, S.K., Yoshino, J., Le, T. Q., Lin, S.J., Sun, S.-W., Cross, A. H., et al. Demyelination increases radial diffusivity in corpus callosum of mouse brain. NeuroImage 2005; 26:132–140.

Tavor, I., Yablonski, M., Mezer, A., Rom, S., Assaf, Y., and Yovel, G. Separate parts of occipito-temporal white matter fibers are associated with recognition of faces and places. NeuroImage 2014; 86:123–130.

Taylor, P. N., Han, C. E., Schoene-Bake, J.C., Weber, B., and Kaiser, M. Structural connectivity changes in temporal lobe epilepsy: Spatial features contribute more than topological measures. NeuroImage: Clinical 2015; 8:322–328.

Taylor, P. N., Sinha, N., Wang, Y., Vos, S. B., de Tisi, J., Miserocchi, A., et al. The impact of epilepsy surgery on the structural connectome and its relation to outcome. NeuroImage: Clinical 2018; 18:202–214.

Thomas, C., Avidan, G., Humphreys, K., Jung, K. J., Gao, F., and Behrmann, M. Reduced structural connectivity in ventral visual cortex in congenital prosopagnosia. Nature Neuroscience 2009; 12:29–31.

Veersema, T. J., van Schooneveld, M. M., Ferrier, C. H., van Eijsden, P., Gosselaar, P. H., van Rijen, P. C., et al. Cognitive functioning after epilepsy surgery in children with mild malformation of cortical development and focal cortical dysplasia. Epilepsy and Behavior 2019; 94:209–215.

Via, E., Zalesky, A., Sanchez, I., Forcano, L., Harrison, B. J., Pujol, J., Fernandez-Aranda, F., et al. Disruption of brain white matter microstructure in women with anorexia nervosa. Journal of Psychiatry and Neuroscience 2014; 39:367–375.

Vicari, S., Albertoni, A., Chilosi, A. M., Cipriani, P., Cioni, G., and Bates, E. Plasticity and reorganization during language development in children with early brain injury. Cortex 2000; 36:31–46.

Wakana, S., Caprihan, A., Panzenboeck, M. M., Fallon, J. H., Perry, M., Gollub, R. L., et al. Reproducibility of quantitative tractography methods applied to cerebral white matter. NeuroImage, 2007; 36:630– 644.

Wheeler-Kingshott, C. A. and Cercignani, M. About “axial” and ”radial” diffusivities. Magnetic Resonance in Medicine 2009; 61:1255–1260.

Xu, J., Rasmussen, I.-A. J., Lagopoulos, J., and Haberg, A. (2007). Diffuse axonal injury in severe traumatic brain injury visualized using high-resolution diffusion tensor imaging. Journal of Neurotrauma, 24(5):753–765.

Yeh, F.C., Verstynen, T. D., Wang, Y., Fernandez-Miranda, J. C., and Tseng, W.Y. I. Deterministic diffusion fiber tracking improved by quantitative anisotropy. PLoS ONE 2013; 8:e80713.

Zhang, W., Muravina, V., Azencott, R., Chu, Z. D., and Paldino, M. J. Mutual Information Better Quantifies Brain Network Architecture in Children with Epilepsy. Computational and Mathematical Methods in Medicine 2018; 2018:6142898.

Zhu, T., Zhong, J., Hu, R., Tivarus, M., Ekholm, S., Harezlak, J., et al. Patterns of white matter injury in HIV infection after partial immune reconstitution: A DTI tract-based spatial statistics study. Journal of NeuroVirology 2013; 19:10–23.

Figure Legends

Figure 1: ILF and IFOF in patients with VOTC resections. ILF and IFOF in exemplar control and patients with VOTC resections to their right hemisphere (RH) and left hemisphere (LH). Anatomical images show the resection site in each patient. Both contralesional and ipsilesional tracts were present in most patients, except for right (ipsilesional) ILF and IFOF in KQ, and left (ipsilesional) IFOF in SN. Ages shown for patients are at time of data acquisition.

Figure 2: Group comparison of microstructural indices between patients and controls. Results of permutation testing of mean microstructural indices of the (A) ILF and (B) IFOF. There were significant group differences at $\alpha = 0.05$ between controls and patients (red dots) for all measures in ipsilesional ILF but only in RD for the IFOF. Both contralesional tracts had group differences of $p > 0.11$ across all microstructural indices. Patient data were compared to the mean of the indices of both hemispheres in controls (top rows) or to indices from either hemisphere (2nd and 3rd rows). Black vertical lines indicate upper and lower 2.5th percentile of the null distribution (gray histogram).

Figure 3: Microstructural indices of the ILF. (A). Anteroposterior profiles of FA, AD, and RD in an exemplar control and in patients with resections to their VOTC. Shaded regions indicate extent of resection. (B). Single-subject comparisons against normative group values (n=15) showed significant differences between ipsilesional and corresponding ILF in controls only for values in the segment corresponding to the resection in each patient. Shaded areas indicate patients with posterior resection, white areas indicate patients with anterior resection. p-values uncorrected for multiple comparisons: $*p < 0.05$, $** p < 0.01$, $*** p < 0.001$.

Figure 4: Microstructural indices of the IFOF. (A). Anteroposterior profiles of FA, AD, and RD in an exemplar control and in patients with resections to their VOTC. Shaded regions indicate extent of resection. (B). Single-subject comparisons against normative group values showed significant differences between ipsilesional and corresponding IFOF in controls only for values in patients with posterior resection. Shaded areas indicate patients with posterior resection, white areas indicate patients with anterior resection. p-values uncorrected for multiple comparisons: $*p < 0.05$, $** p < 0.01$, $*** p < 0.001$.

Figure 5: ILF and IFOF in children with resections outside VOTC. Microstructural indices of the (B) ILF and (C) IFOF in patients with resections outside their VOTC. There were no single-subject level differences to control values for any of the indices of bisected tracts, all $|t|<1.23$, all $p>0.24$. Same colors and orientation as in Fig. 1.

Figure 1.

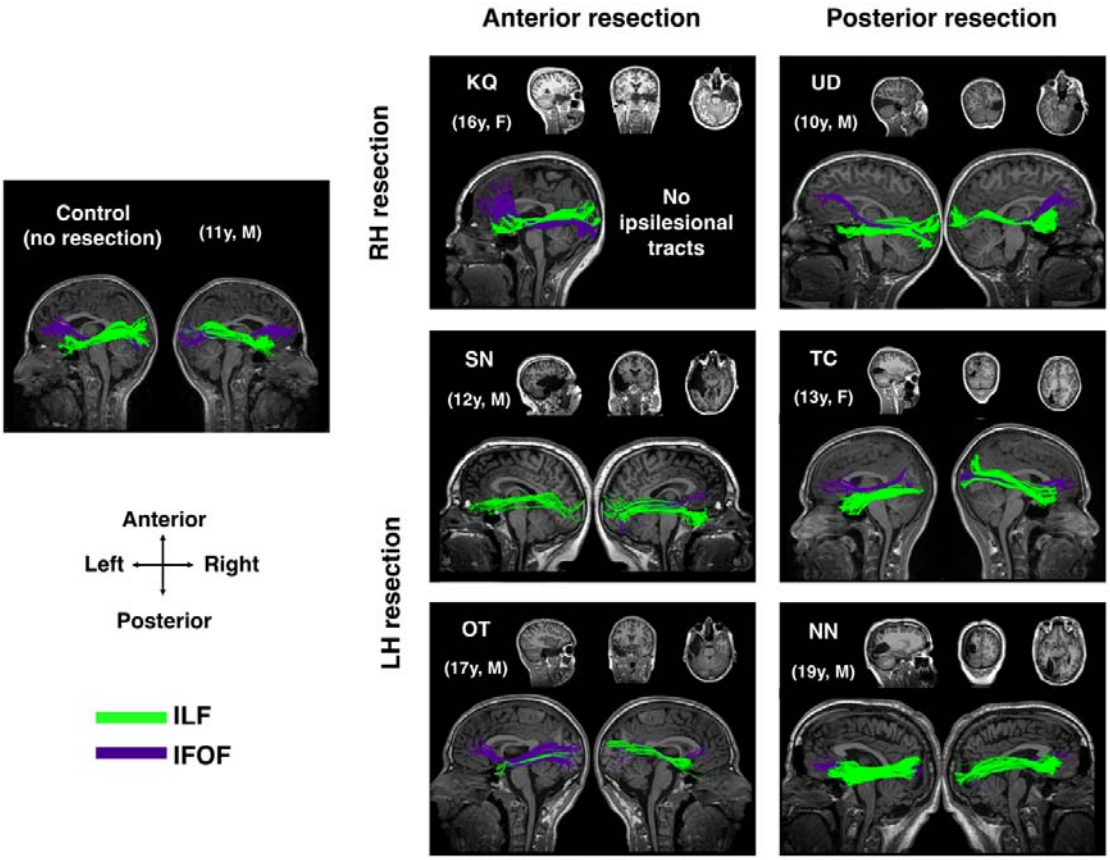
Anterior resection
Posterior resection
RH resection
LH resection
Control
(no resection)
(11y, M)
KQ
(16y, F)
No
ipsilesional
tracts
UD
(10y, M)
SN
(12y, M)
TC
(13y, F)
OT
(17y, M)
NN
(19y, M)
Anterior
Left
Right
Posterior
ILF
IFOF

Figure 2.

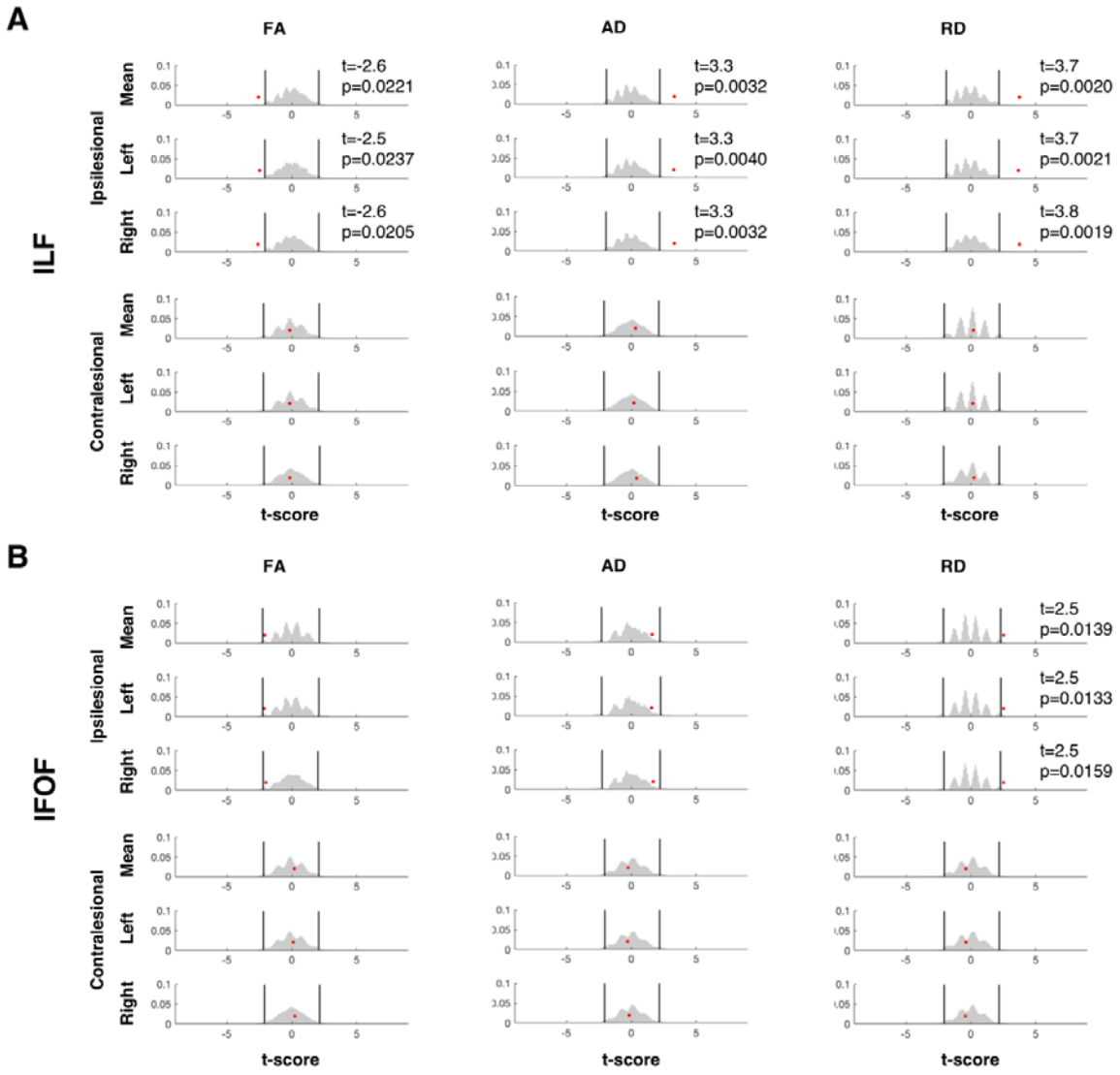
A
ILF
FA
AD
RD
Ipsilesional
Contralesional
Mean
Left
Right
t=-2.6
p=0.0221
t=-2.5
p=0.0237
t=-2.6
p=0.0205
t=3.3
p=0.0032
t=3.3
p=0.0040
t=3.3
p=0.0032
t=3.7
p=0.0020
t=3.7
p=0.0021
t=3.8
p=0.0019
t-score
B
IFOF
t=2.5
p=0.0139
t=2.5
p=0.0133
t=2.5
p=0.0159

Figure 3.

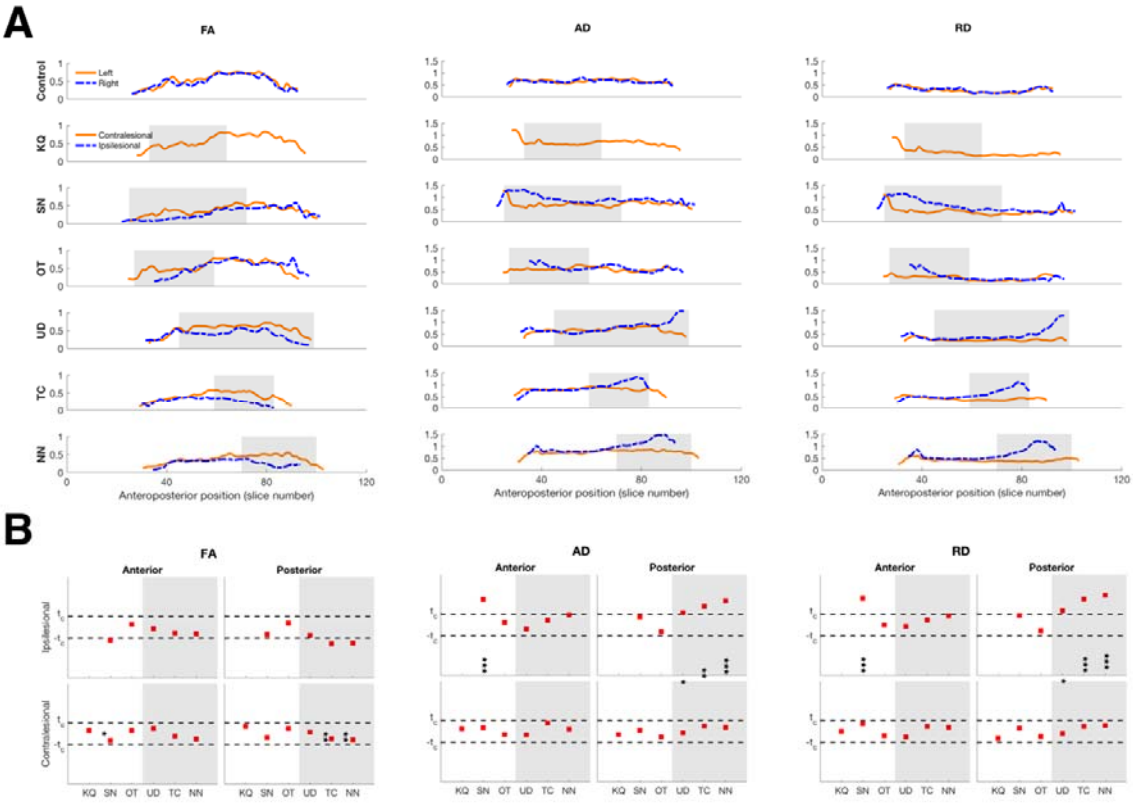
A
FA
AD
RD
Control
KQ
SN
OT
UD
TC
NN
Left
Right
Contralesional
Ipsilesional
Anteroposterior position (slice number)
B
Anterior
Posterior
Ipsilesional
Contralesional
KQ SN OT UD TC NN

Figure 4.

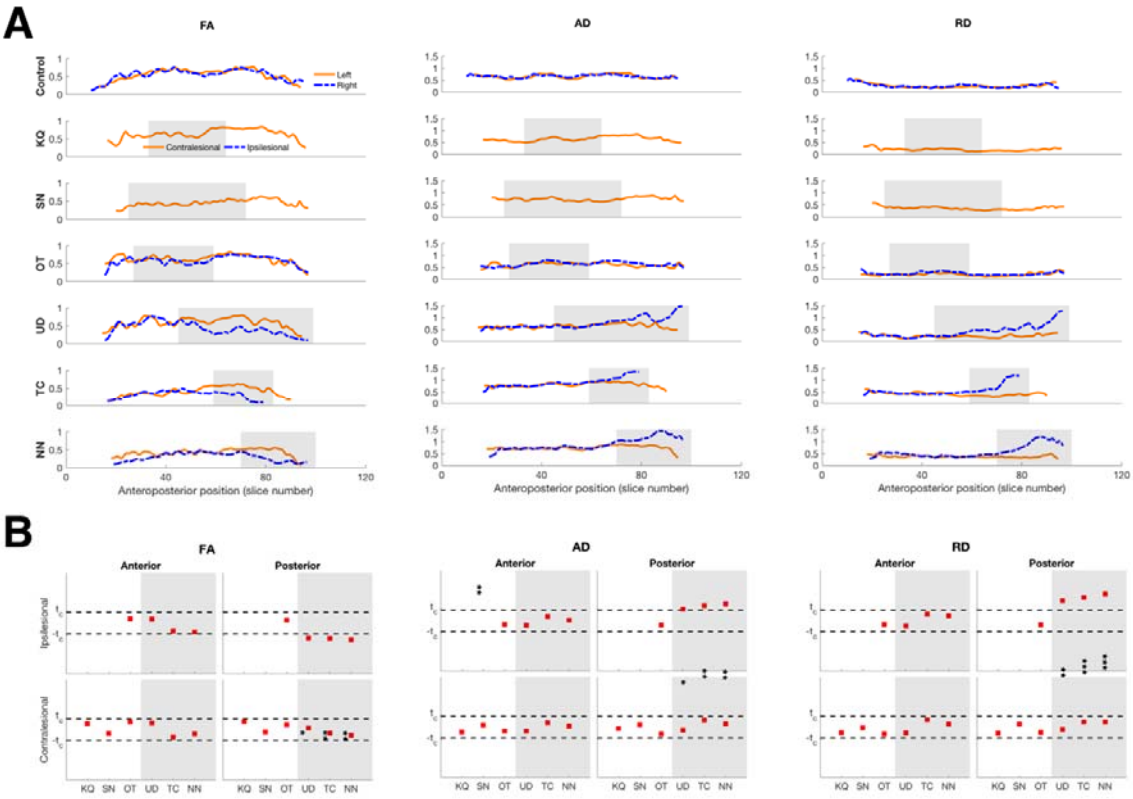
A
FA
AD
RD
Control
KQ
SN
OT
UD
TC
NN
Left
Right
Contralesional
Ipsilesional
Anteroposterior position (slice number)
B
Anterior
Posterior
Ipsilesional
Contralesional
KQ SN OT UD TC NN

Figure 5.

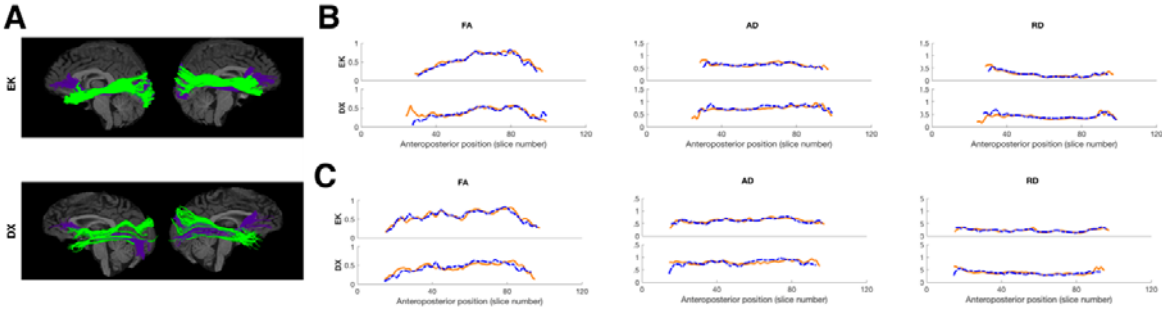
A
EK
DX
B
FA
AD
RD
EK
DX
Anteroposterior position (slice number)
C
FA
AD
RD
EK
DX
Anteroposterior position (slice number)

Table 1. Surgery and data acquisition history of patients.

Patient	**Surgical Procedure**	**Age at resection**	**Time between resection & MRI scan**	**Category selective ROI***
KQ	Right anterior temporal lobectomy and hippocampectomy	15y, 10m	5m	None missing
SN***	Evacuation of left temporal hematoma	1d	12y, 6m	Missing, L: VWFA**
OT	Left temporal lobectomy with preservation of mesial structures, gross total resection of left mesial temporal dysembryoplastic neuroepithelial tumour (DNET)	13y, 4m	4y, 3m	None missing
UD	Right occipital and posterior temporal lobectomy with resection of inferomesial temporal DNET	6y, 9m	4y, 3m	Missing, R: EVC, FFA, PPA, LOC
TC	Left parietal and occipital lobectomy	13y, 3m	8m	Mising, L: EVC, FFA, PPA, LOC, VWFA**
NN	Left occipital lobectomy, left posterior temporal and left parietal corticectomy	15y, 8m	3y, 7m	Missing, L: EVC, PPA, LOC, VWFA
EK	Gross total resection of right frontal neuroglial/gliotic lesion	17y, 1m	8m	None missing
DX***	Left frontal corticectomy with resection of focal cortical dysplastic lesion	15y, 4m	3m	None missing

∗ Category selectivity was defined in (Liu *et al*., 2019) and, in each individual, nine regions were identified where possible: bilateral early visual cortex (EVC), bilateral fusiform face area (FFA), bilateral parahippocampal place area (PPA), bilateral lateral occipital cortex (LOC), and left visual word form area (VWFA).

∗∗ SN's and TC's VWFA were localized in the right hemisphere.

∗∗∗ Category selectivity in patients SN and DX has not been documented previously, but their regions of interest are presented in the supplementary materials (Figs. A.1 and A.2).

Table 2. Comparison of graph-theoretic measures between patients and controls.

Patient	Transitivity	Modularity	Characteristic path length	Efficiency
KQ	t=-1.8, p>0.08	**t=3.0, p<0.01**	**t=2.9, p<0.05**	**t=-2.4, p<0.05**
SN	t=1.6, p>0.13	t=-1.5, p>0.15	t=-1.9, p>0.08	t=1.9, p>0.07
OT	t=-0.7, p>0.50	t=0.7, p>0.40	t=1.0, p>0.33	t=-1.0, p>0.30
UD	t=-1.1, p>0.20	t=0.7, p>0.50	**t=2.5, p<0.05**	**t=-2.2, p<0.05**
TC	t=-0.7, p>0.40	t=-0.7, p>0.40	t=-0.5, p>0.60	t=0.5, p>0.60
NN	t=1.4, p>0.10	t=-1.5, p>0.10	t=-1.7, p>0.10	t=1.7, p>0.10
EK	t=-0.7, p>0.40	t=-0.3, p>0.70	t=1.3, p>0.20	t=-1.3, p>0.20
DX	t=1.9, p>0.07	t=-1.5, p>0.10	t=-1.7, p>0.10	t=1.7, p>0.10

Comparison used single subject t-tests. Values in bold: $p < 0.05$. p-values uncorrected for multiple comparisons.